

# Improving the phase super-sensitivity of squeezing-assisted interferometers by squeeze factor unbalancing

Mathieu Manceau<sup>1</sup>, Farid Khalili<sup>3</sup> and Maria Chekhova<sup>1,2,3</sup>

<sup>1</sup>Max-Planck-Institute for the Science of Light, Erlangen, Germany

<sup>2</sup>University of Erlangen-Nürnberg, Staudtstrasse 7/B2, 91058 Erlangen, Germany

<sup>3</sup>Faculty of Physics, M V Lomonosov Moscow State University, Moscow, Russia

The sensitivity properties of an SU(1,1) interferometer made of two cascaded parametric amplifiers, as well as of an ordinary SU(2) interferometer preceded by a squeezer and followed by an anti-squeezer, are theoretically investigated. Several possible experimental configurations are considered, such as the absence or presence of a seed beam, direct or homodyne detection scheme. In all cases we formulate the optimal conditions to achieve phase super-sensitivity, meaning a sensitivity overcoming the shot-noise limit. We show that for a given gain of the first parametric amplifier, unbalancing the interferometer by increasing the gain of the second amplifier improves the interferometer properties. In particular, a broader super-sensitivity phase range and a better overall sensitivity can be achieved by gain unbalancing.

PACS numbers: 8.67.Bf,42.50.Ar,78.55.Cr,79.20.Fv

## I. INTRODUCTION

Estimating the phase of light is one of the most important tasks in optics. It is the basic tool in many fields, from spectroscopy to the gravitational wave detection<sup>1</sup>. A straightforward way to assess an optical phase shift is to use an interferometer. The phase sensitivity of an interferometer has fundamental bounds, given by the quantum properties of light. In particular, in the most basic case of a coherent quantum state, the phase sensitivity is

$$\Delta\phi_{\text{SNL}} = \frac{1}{2\sqrt{N}}, \quad (1)$$

where  $N$  is the mean photon number<sup>2</sup>. This restriction is known as the shot noise limit (SNL), due to the Poissonian photon statistics of the coherent quantum state.

It is known that the SNL can be overcome by using more advanced sources of light. In fact, the ultimate phase sensitivity achievable according to quantum mechanics is much better than the SNL — it is given by the Heisenberg limit (HL),

$$\Delta\phi_{\text{HL}} \sim \frac{1}{2N}, \quad (2)$$

which is named so because it could be considered as a consequence of the Heisenberg uncertainty relation for the number of quanta and the phase<sup>3</sup>,

$$\Delta N \Delta\phi \geq \frac{1}{2}. \quad (3)$$

$N$  is non-negative, therefore,  $\Delta N \leq N$ , which gives (2).<sup>4</sup>

The ultimate limit for the phase sensitivity can be obtained using the Rao-Cramer approach<sup>5</sup>. It has the form of the uncertainty relation (3), but with a different meaning of  $\Delta\phi$  — now it is a phase shift imposed by some external agent, and not the variance of the (non-existing) phase operator. This limit assumes that some optimal measurement procedure on the outgoing light is used. Whether this procedure can be implemented in practice is another issue. However, it is known

that at least Gaussian quantum states of light, if fed into certain interferometers, can saturate the Rao-Cramer bound in the ideal lossless case<sup>6–9</sup>.

It was shown by direct calculations that the sensitivity (2) can be achieved using exotic quantum states like Pegg-Barnett<sup>10</sup> or NOON<sup>11</sup> ones. However, generation of these states for  $N \gg 1$  is impossible with the current state-of-the-art technologies. Another, much more realistic class of quantum states, namely squeezed states, was explored in the pioneering work by C. Caves<sup>6</sup>. In the reasonable case of not very strong squeezing,  $e^{2r} \ll N$ , where  $r$  is the squeeze factor, the phase sensitivity corresponds to the “improved” SNL:

$$\Delta\phi_{\text{sqz}} = \frac{e^{-r}}{2\sqrt{N}}. \quad (4)$$

In the (hypothetic) case of very strong squeezing,  $e^{2r} \sim N$ ,  $\Delta\phi_{\text{sqz}}$  asymptotically approaches the Heisenberg limit (2).

Recently, reduction of the noise below the SNL by means of squeezed-states injection was demonstrated in kilometers-scale interferometers of laser gravitational-wave detectors GEO-600<sup>12</sup> (which continues to routinely operate in this regime<sup>13</sup>) and LIGO<sup>14</sup>. A 10 dB squeezed light source was used in these experiments. However, the achieved sensitivity gain was much smaller (about 3 dB and 2 dB, respectively). The reason for such modest effect of squeezing on the phase sensitivity is the fragility of squeezed light to optical losses, both inside the interferometer (the *internal losses*) and in the output optical path, including the photodetectors’ quantum inefficiency (the *external losses*). It should be noted that in the state-of-the-art interferometers and, in particular, in laser gravitational-wave detectors, it is the external losses that apply most severe limitations on the sensitivity (see the loss budget analysis in<sup>12,14</sup>).

In the same paper<sup>6</sup>, C. Caves proposed to amplify the signal, as well as the noise component that is in phase with the signal, by means of a second (anti)squeezer located in the output path of the interferometer. In Fig. 1, implementation of this idea for a Mach-Zehnder interferometer is shown. This additional squeezer does not affect the signal-to-noise ratio

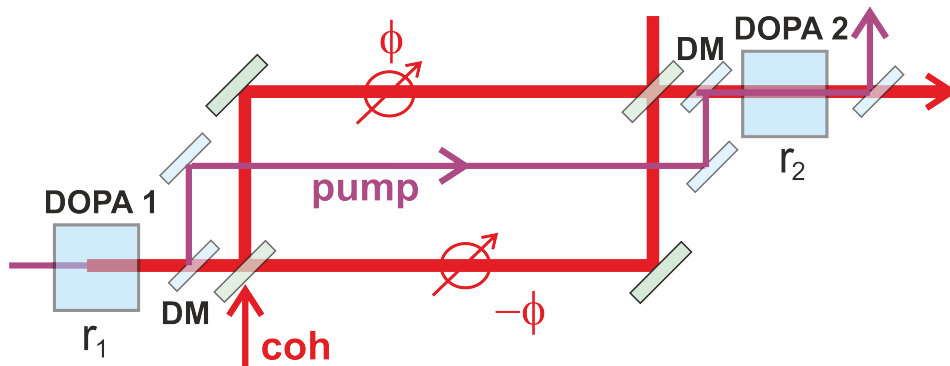


FIG. 1. A linear interferometer preceded by a squeezer (degenerate optical parametric amplifier, DOPA1, with the squeeze factor  $r_1$ ) and followed by an anti-squeezer (DOPA2), with the squeeze factor  $r_2$ . The pump path can be arranged by using dichroic mirrors DM.

(SNR) associated with the internal losses and the corresponding noise, because both the signal and this noise are equally amplified or de-amplified. At the same time, amplification of the signal by the output anti-squeezer suppresses the influence of the external losses on the phase sensitivity. It is important to note that the decrease of  $\Delta\phi$  is not accompanied by an increase of  $\Delta N$ , see Eq. (3), because the optical quantum state inside the interferometer is obviously not affected by the output anti-squeezer. This means that the phase measurement indeed becomes more efficient, that is, closer to the Rao-Cramer bound.

In 1986, an ingenious scheme, the so-called *SU(1,1) interferometer*, was proposed by Yurke et al.<sup>7</sup> It can be viewed as a further development of the idea of Fig. 1, with the beam-splitters “fused” together with the corresponding squeezers. Two versions of this scheme were proposed, based on the degenerate (DOPA) and non-degenerate (NOPA) optical parametric amplifiers, shown in Fig. 2a,b, respectively. Here, light generated or amplified in the first OPA is amplified or de-amplified in the second one, depending on the phase shifts  $\phi_{p,s,i}$  introduced in the pump, signal, and idler channels, respectively. The term *SU(1,1)* comes from the fact that this interferometer performs Bogolyubov (related to the *SU(1,1)* group) transformations of the optical fields (note that the *SU(1,1)* interferometer is a special case of a broader class of nonlinear interferometers<sup>15</sup>). Correspondingly, for the ordinary linear interferometers, performing an *SU(2)* transformation, the term *SU(2) interferometer* was coined in<sup>7</sup>; we adopt this terminology here.

Later, Plick et al. showed<sup>16</sup> that the performance of an *SU(1,1)* interferometer can be improved by seeding it with coherent light.

The influence of the optical losses on the performance of this scheme was calculated by Marino et al.<sup>17</sup> who explicitly showed it to be highly immune to external losses. This result is well expected, taking into account that the *SU(1,1)* interferometer uses the same squeezing/antisqueezing principle as the scheme of C. Caves.

Recently, an *SU(1,1)* interferometer has been implemented using two cascaded four-wave mixers (FWM), and an enhancement in the fringe intensity compared to a linear interferometer without squeezing was demonstrated<sup>18,19</sup>. In Ref.<sup>20</sup>,

about 4 dB enhancement of the phase sensitivity in an *SU(1,1)* interferometer was achieved. Phase locking aimed at working at the optimum sensitivity point of such an interferometer was also demonstrated<sup>21</sup>.

Evidently, the signs of the squeeze factors  $r_1, r_2$ , given by the parametric gain values of the first and the second OPAs, both in the linear (Fig. 1) and non-linear (Fig. 2) interferometers, have to be opposite,  $r_1 r_2 < 0$ . Their absolute values could be equal (the balanced case,  $|r_1| = |r_2|$ ) or different (the unbalanced case,  $|r_1| \neq |r_2|$ ). Typically in the previous works, starting from the initial paper<sup>6</sup>, the balanced case was considered theoretically and implemented experimentally. This is a necessary requirement in the case of FWM, as the mode structure of an FWM OPA considerably depends on the gain<sup>22</sup>. However, it does not have to be the case in the other realizations of the parametric amplifiers. In particular, it was shown in<sup>23</sup> that the shapes of spatial and temporal modes of the parametric amplifiers based on high-gain parametric down-conversion<sup>24,25</sup> can be considered as gain-independent. The unbalanced regime of an *SU(1,1)* interferometer was considered in Ref.<sup>26</sup>, with the conclusion that the best regime is the balanced or close to the balanced one. However, this conclusion was based on a non-optimal detection procedure, with only one of the two output beams measured.

In this paper, we consider the unbalanced regime in detail and show that if a proper detection procedure is used, then indeed the sensitivity for both *SU(2)* and *SU(1,1)* interferometers increases with the output squeezing strength. We focus here on “practical” schemes involving Gaussian (coherent or squeezed) states of light and available detection methods. The general introduction into the field can be found *e.g.* in the review article<sup>27</sup>.

An important feature of the phase estimation is that it is essentially a relative measurement and assumes the existence of some phase reference point in the form of *e.g.* the local oscillator phase or the optical pump phase. (Probably the only exception is a non-squeezed two-arms linear interferometer with the direct photocounting at the output(s).) This phase reference beam could be viewed as a problem in practical realizations of phase-supersensitive schemes. Indeed, the photon number  $N$  entering the expressions for SNL and HL is actually limited by various undesirable effects of the optical power



ference between the arms,  $\phi_1 = \phi$  and  $\phi_2 = -\phi$ . However, in the real-world interferometers (laser gravitational-wave detectors can be mentioned as the most conspicuous example), the bright port is contaminated by the laser technical noises and therefore this possibility can not be considered as a practical one. Here we limit ourselves to the antisymmetric case only.

Following the initial proposals<sup>6,7</sup>, both here and in the following section, devoted to the SU(1,1) case, we assume that both squeezers are in phase with the coherent light. In this case, it is natural to set the corresponding phases equal to zero. In particular, this means that  $\alpha$  is real. We assume also the following signs of the squeeze factors:  $r_1 > 0$ ,  $r_2 < 0$ .

We show in B that the phase sensitivity in this case is

$$(\Delta\phi)^2 = (\Delta\phi_{\min})^2 + K \tan^2 \phi, \quad (5)$$

where

$$\Delta\phi_{\min} = \frac{1}{2\alpha} \sqrt{e^{-2r_1} + \frac{1-\mu}{\mu} + \frac{1-\eta}{\mu\eta} e^{-2|r_2|}}, \quad (6)$$

is the best sensitivity achieved at  $\phi = 0$ , and

$$K = \frac{1}{4\alpha^2} \left( \frac{1}{\mu} + \frac{1-\eta}{\mu\eta} e^{-2|r_2|} \right) \quad (7)$$

is the factor defining the sensitivity deterioration with the increase of  $\phi$ . In Eqs. (5,7),  $\mu$  and  $\eta$  are the quantum efficiencies corresponding to the internal and the external losses, respectively. One can easily see that at  $|r_2| \rightarrow \infty$ , the terms in  $\Delta\phi_{\min}$  and  $K$  associated with the external losses vanish.

Note that despite the different detection procedures, we obtained virtually the same result as in<sup>6</sup>, up to the notation and taking into account that the condition  $r_1 = |r_2|$  was assumed in that paper. The characteristic dependence of the phase sensitivity on the losses in Eqs. (6, 7), as well as in other similar equations below in this paper, actually corresponds to the fundamental bound on lossy interferometry predicted in<sup>29-31</sup> and observed experimentally in<sup>32</sup>.

We consider first the optimization of  $\Delta\phi_{\min}$  with respect to the input squeezing strength  $r_1$  for a given mean number of photons used for the measurement,

$$N = \alpha^2 + \sinh^2 r_1, \quad (8)$$

in the ideal lossless case  $\mu = \eta = 1$ . In this case, the minimum of (6) in  $r_1$  occurs for

$$e^{2r_1} = 2N + 1, \quad (9)$$

and is equal to

$$(\Delta\phi_{\min})^2 = \frac{1}{4N(N+1)}. \quad (10)$$

This means that the setup shown in Fig. 1 could reach the HL in the ideal lossless scenario.

In addition to  $\Delta\phi_{\min}$ , another important figure of merit is the phase range  $\Delta$  where the sensitivity exceeds the SNL. We will

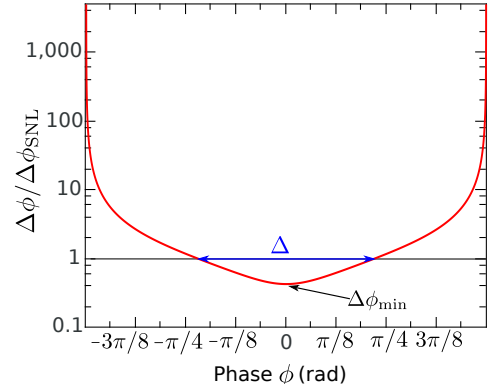


FIG. 3. Phase sensitivity of an SU(2) interferometer preceded by a squeezer and followed by an antisqueezer (Fig.1), as a function of the phase shift in the interferometer, for the parameters given by (16, 17) and a homodyne detection. The best phase sensitivity  $\Delta\phi_{\min}$  is obtained at  $\phi_0 = 0$ . The supersensitive phase range  $\Delta$ , for which  $\Delta\phi < \Delta\phi_{\text{SNL}}$ , is shown in blue.

further call it the supersensitive phase range. It follows from (5) that it is equal to

$$\Delta = 2 \arctan \sqrt{\frac{(\Delta\phi_{\text{SNL}})^2 - (\Delta\phi_{\min})^2}{K}}. \quad (11)$$

For a high-precision measurement,  $\Delta$  approaches a simple asymptotic value. Suppose that

$$(\Delta\phi_{\min})^2 \ll (\Delta\phi_{\text{SNL}})^2. \quad (12)$$

The necessary conditions for this are

$$1 - \mu \ll 1, \quad (1 - \eta)e^{-2|r_2|} \ll 1. \quad (13)$$

Note also that in the reasonable real-world scenarios,

$$\alpha^2 \gg \sinh^2 r_1 \Rightarrow N \approx \alpha^2. \quad (14)$$

Below we assume this condition for all relevant cases. In particular, it follows from (14) that  $K \approx (\Delta\phi_{\text{SNL}})^2$  and

$$\Delta \approx \frac{\pi}{2} \quad (15)$$

Fig. 3 shows the phase sensitivity  $\Delta\phi$  given by Eq. 5, normalized to the shot-noise-limited phase sensitivity  $\Delta\phi_{\text{SNL}}$ , as a function of the phase  $\phi$ , for the following set of parameters:

$$r_1 = 1.15, \quad \mu = 0.90, \quad (16)$$

$$|r_2| = 3, \quad \eta = 0.3. \quad (17)$$

The horizontal line in Fig. 3 marks the SNL phase sensitivity. One can see from this plot that for the values (16, 17), which could be considered as “reasonably optimistic” ones,  $\Delta$  is indeed very close to  $\pi/2$ .

Now consider the dependence of the best phase sensitivity  $\Delta\phi_{\min}$  (6) and the supersensitive phase range  $\Delta$  (11) on  $r_2$  and

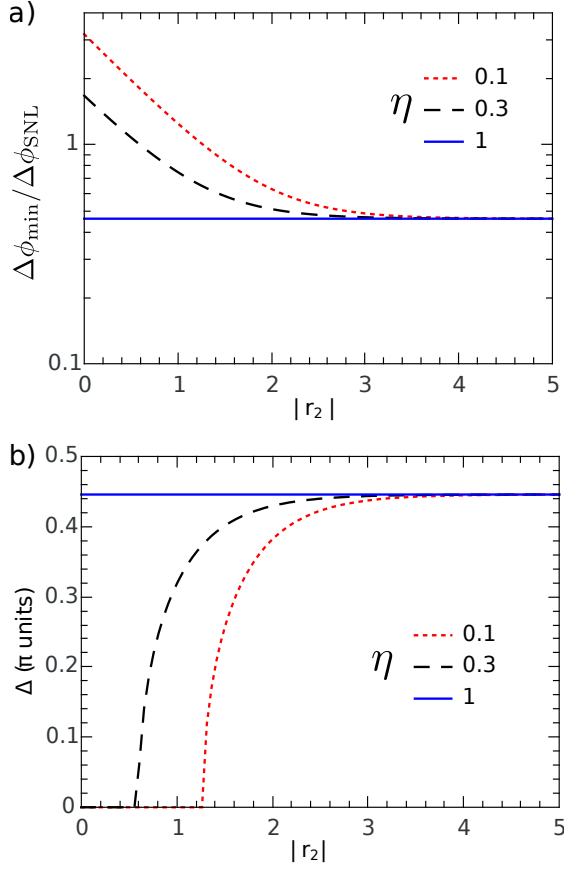


FIG. 4. Optimal sensitivity  $\Delta\phi_{\min}$  normalized to  $\Delta\phi_{\text{SNL}}$  (a) and the supersensitive phase range (b) of an SU(2) interferometer preceded by a squeezer and followed by an antisqueezer as functions of the gain  $r_2$  of the second amplifier for various values of the detection efficiency  $\eta$ : blue line  $\eta = 1$ , black dashed line  $\eta = 0.3$  and red dotted line  $\eta = 0.1$ . The gain of the first amplifier  $r_1$  and the internal transmission  $\mu$  are given by (16).

$\eta$ . In Fig.4, the ratio  $\Delta\phi_{\min}/\Delta\phi_{\text{SNL}}$  and  $\Delta$  are plotted as functions of  $r_2$  for various values of  $\eta$ , from the extremely lossy case corresponding to  $\eta = 0.1$  to no external losses. The values of  $r_1$  and  $\mu$  are given by (16). In all cases, the external losses can be overcome by increasing the parametric gain of the output amplifier. The sensitivity corresponding to the ideal detection ( $\eta = 1$ ) case can be recovered if

$$e^{-2|r_2|} \ll \frac{\eta}{1-\eta} (\mu e^{-2r_1} + 1 - \mu), \quad (18)$$

more external losses requiring more parametric gain as one can see in Fig.4.

Also, an increase in the detection losses leads to a smaller super-sensitive phase range until the super-sensitivity eventually disappears. By increasing the gain of the second squeezer, one improves not only the sensitivity as seen previously but also the supersensitive phase range  $\Delta$ . A supersensitive phase range as broad as in the case of lossless detection can always be retrieved by increasing the parametric gain of the second amplifier.

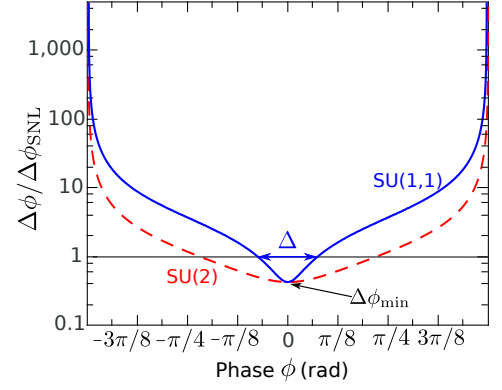


FIG. 5. Phase sensitivity of a seeded SU(1,1) interferometer (blue line) with homodyne detection (Fig.2), as a function of the phase shift in the interferometer, for the parameters from (16, 17) and a homodyne detection. The best phase sensitivity  $\Delta\phi_{\min}$  is obtained at  $\phi_0 = 0$ . The supersensitive phase range  $\Delta$  for which  $\Delta\phi < \Delta\phi_{\text{SNL}}$  is shown (blue arrow). For comparison, the phase sensitivity of an SU(2) interferometer (red dashed line) from Fig.3 is plotted as well.

### III. SEEDED SU(1,1) INTERFEROMETER WITH HOMODYNE DETECTION

#### A. Degenerate interferometer

We now consider an SU(1,1) interferometer made of two cascaded OPAs. We start with the simpler degenerate case shown in Fig. 2a. We suppose here that a coherent seed beam is injected into the first DOPA, and homodyne detection is used at the output of the interferometer.

Calculations given in C 2 for a phase shift  $\phi = \phi_s - \phi_p/2$  yield in this case that the equation for the phase sensitivity again has the form (5), with the same equation for  $\Delta\phi_{\min}$  (6), but with a different factor  $K$ :

$$K = \frac{1}{4\alpha^2} \left( e^{2r_1} + \frac{1-\mu}{\mu} + \frac{1-\eta}{\mu\eta} e^{-2|r_2|} \right). \quad (19)$$

In all these equations for the SU(1,1) interferometer,  $\alpha$  has the meaning of the classical amplitude inside the interferometer, which is  $e^{r_1}$  times stronger than the seed amplitude. The term  $e^{2r_1}$  in (19) originates from the amplitude (anti-squeezed) light quadrature and noticeably reduces the supersensitive phase range of this scheme in comparison with the linear interferometer, see Eq. (20). Fig.5 shows the phase sensitivity  $\Delta\phi$  given by Eq. (5), with  $K$  given by Eq.(19), as a function of the phase  $\phi$ . The sensitivity is normalized to the shot-noise-limited phase sensitivity  $\Delta\phi_{\text{SNL}}$  and the parameters from (16) and (17) are used.

The mean number of photons used for the measurement in this case is also described by equation (8). Therefore, the optimization of the best phase sensitivity  $\Delta\phi_{\min}$  again gives the HL (10).

Using the same approach as in Sec. II, we can also calculate the asymptotic value of  $\Delta$  for the high-precision measurement case. It is easy to show that it is equal to

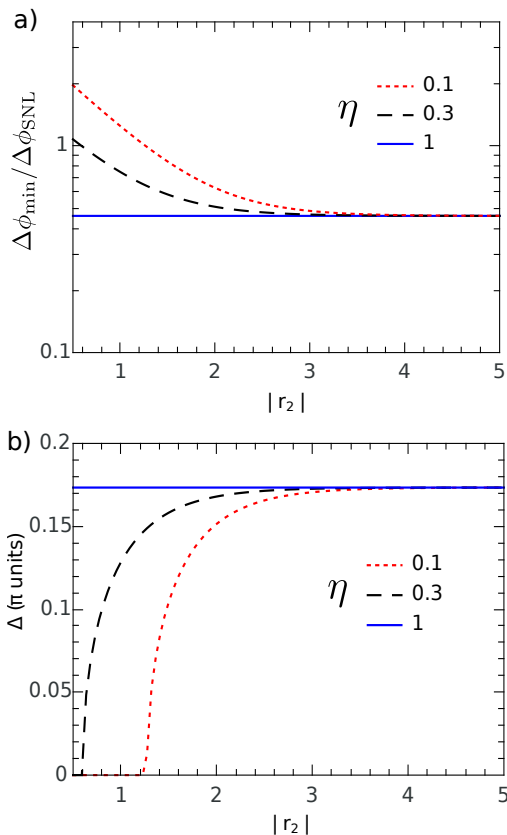


FIG. 6. Optimal phase sensitivity normalized to the SNL (a) and the supersensitive phase range (b) of a seeded degenerate SU(1,1) interferometer with homodyne detection as functions of the gain  $r_2$  of the second amplifier for various values of the detection efficiency  $\eta$ : blue line  $\eta = 1$ , black dashed line  $\eta = 0.3$  and red dotted line  $\eta = 0.1$ . The gain of the first amplifier  $r_1$  and the internal transmission  $\mu$  are given by (16).

$$\Delta \approx 2 \arctan e^{-r_1} \approx 2e^{-r_1} \quad (20)$$

i.e., it is  $\sim e^{r_1}$  times narrower than in the linear interferometer case.

These results are summarized in Fig. 6 showing the phase sensitivity normalized to the shot-noise level and the supersensitive phase range as functions of  $r_2$  for different values of  $\eta$ , with the other parameters given by (16). These results are very similar to the ones calculated for an SU(2) interferometer. The only difference is a narrower supersensitive phase range.

### B. Non-degenerate interferometer

Consider now a non-degenerate SU(1,1) interferometer as in Fig. 2b undergoing a phase shift  $\phi = (\phi_s + \phi_i - \phi_p)/2$ . We show in D that if the signal and the idler arms experience the same phase shifts and have the same optical losses, then this case is equivalent to the one of two independent degen-

erate SU(1,1) interferometers, corresponding to the symmetric (+) and antisymmetric (-) optical modes of the initial non-degenerate interferometer. Here, “independent” means that all optical fields in these modes are uncorrelated. The squeeze factors of the two equivalent DOPAs in the symmetric mode are the same as the ones of the initial NOPAs:  $r_1, r_2$ , respectively. For the antisymmetric-mode equivalent DOPAs, the squeeze factors are  $-r_1$  and  $-r_2$ , respectively.

If two homodyne detectors are placed in the signal and idler output ports of the interferometer in Fig. 2b and they measure the same quadrature, then this equivalence can be extended to the detection procedure as well. In this case, the sum and difference of the photocurrents of the signal and idler outputs correspond to the output signals of the effective symmetric and antisymmetric non-degenerate interferometers. The corresponding phase sensitivities,  $\Delta\phi_+$  and  $\Delta\phi_-$ , are given by equations (5, 6, 19) with inverted signs of the squeeze factors for the antisymmetric-mode interferometer. Correspondingly, the total measurement error is

$$(\Delta\phi)^2 = \left[ \frac{1}{(\Delta\phi_+)^2} + \frac{1}{(\Delta\phi_-)^2} \right]^{-1}. \quad (21)$$

Let us find now the optimal distribution of the number of quanta between the signal and idler modes, assuming a given total number of quanta. It follows from Eq. (D8) that

$$\alpha_s^2 + \alpha_i^2 = \alpha_+^2 + \alpha_-^2, \quad (22)$$

where  $\alpha_{s,i}$  and

$$\alpha_{\pm} = \frac{\alpha_s \pm \alpha_i}{\sqrt{2}} \quad (23)$$

are the classical field amplitudes inside the interferometer in the respective modes. It is evident that if  $\Delta\phi_+ < \Delta\phi_-$ , then all power should be redistributed to the “+” mode, giving  $\alpha_- = 0$ , and if  $\Delta\phi_+ > \Delta\phi_-$ , then to the “-” mode, giving  $\alpha_+ = 0$ . In both cases, the seed inputs have to be balanced:  $|\alpha_s|^2 = |\alpha_i|^2$ , and in both cases,  $\Delta\phi$  takes the form of (5, 6, 19), with  $\alpha^2$  corresponding to the total number of quanta.

Experimentally, the “+” or “-” modes can also be accessed by mixing the two outputs of the interferometer on a beam-splitter. The desired quadrature can then be measured by a single homodyne detector with the local oscillator matching one of these modes at a given output of the beamsplitter.

## IV. SEEDED SU(1,1) INTERFEROMETER WITH DIRECT DETECTION

In many cases, the homodyne detection procedure considered above can be substituted by the simpler measurement of the total output intensity, a *direct detection* scheme. Unlike homodyne detection, it does not require the use of a local oscillator, and it can be applied whenever the measured signal exceeds considerably the detector dark noise. We show here that direct detection is able to provide a sensitivity close to the one of the homodyne detection case. Here and in the next section we limit ourselves to the degenerate case only.



Similar to the schemes considered above, we assume that the first and the second OPAs are tuned in anti-phase to each other:  $r_1 > 0, r_2 < 0$ . However, we suppose that the seed phase inside the interferometer could differ from the squeeze phase by some angle  $\psi$ , that is, the corresponding complex amplitude of the seed has the form of  $\alpha e^{-i\psi}$ , where  $\alpha$  is real.

The degenerate SU(1,1) with the direct detection is considered in C3, with an account for the above assumptions. The resulting equations (C25-C33) for the phase sensitivity are quite cumbersome. Therefore, let us consider some characteristic particular cases.

As in the previous sections, we start with the ideal lossless case  $\mu = \eta = 1$ . Numerical optimization shows that if  $e^{-|r_{1,2}|} \ll 1$ , then the minimum of  $\Delta\phi$  occurs at

$$\phi = -(\phi + \psi) \approx \pm e^{-2|r_2|}, \quad (24)$$

and is

$$\Delta\phi_{\min} = \frac{e^{-r_1}}{2\alpha}. \quad (25)$$

This coincides with the best sensitivity of the homodyne detection cases considered in the previous sections. The mean number of photons used for the measurement in this case is again given by equation (8), therefore, the direct detection scheme can also reach the HL (10).

It follows from Eqs.(C25-C33) that the best sensitivity is achieved at small values of  $\phi$ . By assuming again  $e^{-|r_{1,2}|} \ll 1$ ,

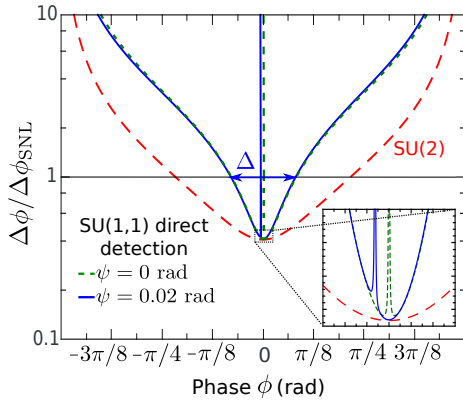


FIG. 7. Phase sensitivity of a seeded SU(1,1) interferometer with direct detection (Fig.2), as a function of the phase shift in the interferometer, for the parameters from (16, 17) and a zoom into the optimized sensitivity region around  $\phi = 0$  in the inset. Different seed phases  $\psi$  are considered. For comparison, the phase sensitivity of an SU(2) interferometer (red dashed line) with homodyne detection from Fig.3 is plotted as well. The best phase sensitivity  $\Delta\phi_{\min}$  is obtained at  $\phi_0 = 0$  if the seed is slightly out of phase,  $\psi \neq 0$ . The supersensitive phase range  $\Delta$ , for which  $\Delta\phi < \Delta\phi_{\text{SNL}}$  is shown by a blue arrow.

Eq. (C25) can be approximated as follows:

$$(\Delta\phi)^2 = \frac{1}{4\alpha^2} \left\{ e^{-2r_1} + \left( \phi + \frac{e^{-4|r_2|}}{\phi + \psi} \right)^2 e^{2r_1} + \frac{1-\mu}{\mu} \left[ 1 + \frac{e^{-8|r_2|}}{(\phi + \psi)^2} \right] + \frac{1-\eta}{\mu\eta} e^{-2|r_2|} \left[ 1 + \frac{e^{-4|r_2|}}{(\phi + \psi)^2} \right] \right\}. \quad (26)$$

Comparison of this equation with Eqs. (5, 6, 19) shows that direct detection provides almost the same performance as homodyne detection and, in particular, results in almost the same supersensitive phase range, approximately  $e^{-r_1}$  smaller than in the SU(2) case:

$$\Delta \approx 2e^{-r_1}. \quad (27)$$

Also, similar to the previous cases, if  $|r_2| \rightarrow \infty$ , then the term containing the external losses vanishes.

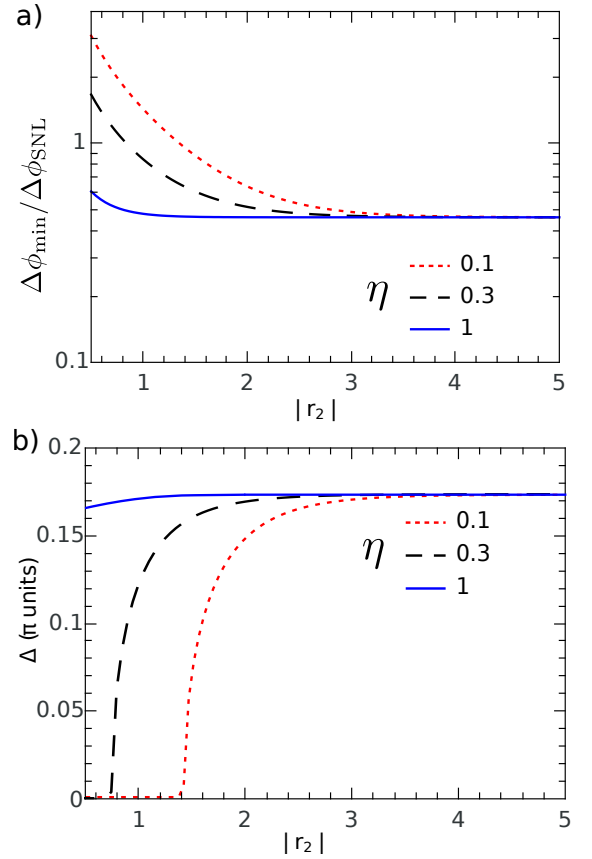


FIG. 8. Optimal phase sensitivity  $\Delta\phi_{\min}$  normalized to  $\Delta\phi_{\text{SNL}}$  (a) and the supersensitive phase range  $\Delta$  (b) of a seeded degenerate SU(1,1) interferometer with direct detection as functions of the gain  $r_2$  of the second amplifier for various values of the detection efficiency  $\eta$ : blue line  $\eta = 1$ , black dashed line  $\eta = 0.3$  and red dotted line  $\eta = 0.1$ . The gain of the first amplifier  $r_1$  and the internal transmission  $\mu$  are given by (16).

However, function (26) has a narrow peak at  $\phi + \psi \rightarrow 0$ , with the width  $\sim e^{-2|r_2|}$ , originating from the absence of phase

sensitivity at this point:

$$\left. \frac{\partial \langle N_f \rangle}{\partial \phi} \right|_{\phi+\psi=0} = 0, \quad (28)$$

see Eq. (C33). This peak divides the supersensitive region into two parts and can be considered as the main drawback of the direct detection scheme compared to the homodyne one.

These results are illustrated by Fig. 7 showing the phase sensitivity normalized to the shot-noise level and by Fig. 8 showing the dependence of the optimal phase sensitivity  $\Delta\phi_{\min}$  and of the supersensitive phase range  $\Delta$  on  $r_2$  and  $\eta$  for the parameters (16).

In Fig. 7 we can see that the phase sensitivity in the direct detection scheme is much similar to the SU(1,1) homodyne case shown in Fig. 5 except for the extra peak denoting the absence of sensitivity for  $\phi + \psi \rightarrow 0$  as explained earlier. In particular, the phase supersensitivity range is the same as in the homodyne detection case when neglecting the small insensitive peak range. The SU(2) homodyne case (red dashed line) is also shown as a reference. Two curves are presented corresponding to two values of the seed phase  $\psi$ . By tuning the value of  $\psi$  the insensitive peak can be moved away from  $\phi = 0$  as follows from the graph. The optimal phase sensitivity  $\Delta\phi_{\min}$  can be improved this way as visible in the inset of Fig.7 which is a zoom into the  $\phi = 0$  region. For the particular case of the parameters (16, 17), the best phase sensitivity corresponds to  $\psi \approx 0.2$  and approaches the lossless limit (25). In Fig. 8a,b we observe the same trend as for the homodyne detection case: by increasing the gain of the second amplifier one can compensate for the effect of external losses on the optimal phase sensitivity and the supersensitivity phase range.

## V. UNSEEDED SU(1,1) INTERFEROMETER WITH DIRECT DETECTION

Finally, we consider the simplest case of an unseeded SU(1,1) interferometer followed by a direct detection. Calculations for this regime are made in C 4; the corresponding phase sensitivity is described by Eqs. (C41-C42), which have a rather sophisticated structure.

The dependence of the phase sensitivity (C41) on the working point  $\phi$  is shown in Fig. 9. The parameters of the interferometer, as in the previous cases, are given by Eqs. (16, 17). One can see that similar to the previous (seeded direct detection) case, the supersensitive region is split into two parts by a narrow peak at  $\phi = 0$ .

It can be also shown that for the strong squeezing case, the optimal working point  $\phi_0$ , which gives the best phase sensitivity, is close to the dark fringe  $\phi = 0$ , although does not exactly coincide with it. Therefore, suppose that  $|\phi| \ll 1$ . Assume also that  $r_1 > 0$ ,  $r_2 < 0$ , which corresponds to the same ‘‘squeezing/antisqueezing’’ procedure that we considered above. In this case, the phase sensitivity is

$$(\Delta\phi)^2 = \frac{1}{2} \left[ \phi^2 + \frac{\cosh 2R + A/2}{|\sinh 2r_1 \sinh 2r_2|} + \frac{\sinh^2 2R + 2(A \sinh^2 R + B)}{4\phi^2 \sinh^2 2r_1 \sinh^2 2r_2} \right], \quad (29)$$

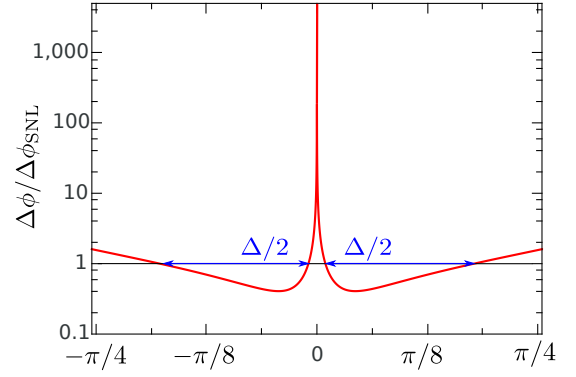


FIG. 9. Phase sensitivity of an unseeded degenerate SU(1,1) interferometer with direct detection as a function of the phase shift for the parameters (16, 17). The supersensitive phase range  $\Delta$  is indicated in the graph.

where

$$R = r_1 + r_2 \quad (30)$$

and the phase-independent factors  $A, B$  are defined by the optical losses and the additional photon-number measurement uncertainty  $\Delta N_d$  introduced by the photcounter, see (C42). This additional measurement uncertainty becomes important only in the unseeded direct detection case, because in this case the number of photons measured by the detector at the dark fringe is relatively small. For homodyne detection and/or seeded schemes, the contribution of this noise can be made arbitrary small by simply increasing the power of the local oscillator and/or seed. Therefore, we did not take it into account in the previous sections.

The minimum of  $\Delta\phi$  in  $\phi$  is achieved at

$$\phi_0^2 = \frac{\sqrt{\sinh^2 2R + 2(A \sinh^2 R + B)}}{2|\sinh 2r_1 \sinh 2r_2|} \quad (31)$$

and is equal to

$$(\Delta\phi_{\min})^2 = \frac{\sqrt{\sinh^2 2R + 2(A \sinh^2 R + B) + \cosh 2R + A/2}}{2|\sinh 2r_1 \sinh 2r_2|}. \quad (32)$$

It is instructive to consider the asymptotic case of (29) for very strong second (anti)squeezing,  $e^{|r_2|} \rightarrow \infty$ . It is easy to see that in this case

$$A \rightarrow \frac{1}{2} \frac{1-\mu}{\mu} e^{2|r_2|}, \quad B \rightarrow \frac{1}{8} \left( \frac{1-\mu}{\mu} \right)^2 e^{4|r_2|}, \quad (33)$$

and

$$(\Delta\phi)^2 = \frac{1}{2} \left\{ \phi^2 + \frac{1}{\sinh 2r_1} \left( e^{-2r_1} + \frac{1-\mu}{2\mu} \right) + \frac{1}{4\phi^2 \sinh^2 2r_1} \left[ e^{-4r_1} + \frac{1-\mu}{\mu} e^{-2r_1} + \left( \frac{1-\mu}{\mu} \right)^2 \right] \right\}. \quad (34)$$



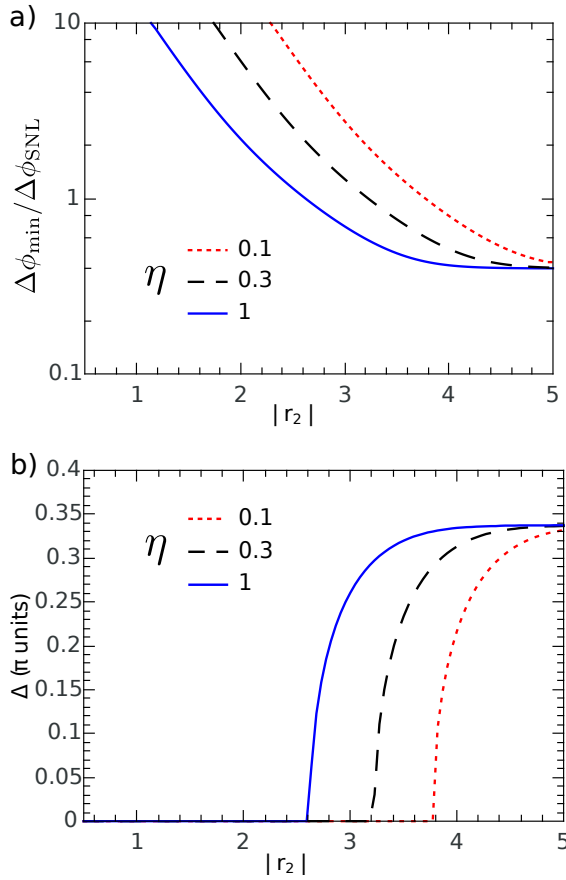


FIG. 10. Optimal phase sensitivity  $\Delta\phi_{\min}$  normalized to  $\Delta\phi_{\text{SNL}}$  (a) and the supersensitive phase range  $\Delta$  (b) of an unseeded degenerate SU(1,1) interferometer with direct detection as functions of the gain  $r_2$  of the second amplifier for various values of the detection efficiency  $\eta$ : blue line  $\eta = 1$ , black dashed line  $\eta = 0.3$  and red dotted line  $\eta = 0.1$ . The gain of the first amplifier  $r_1$  and the internal transmission  $\mu$  are given by (16); the detection noise is  $\Delta N_d = 100$  photons.

Note that all terms originating from the output losses and the detector imperfections are absent in this equation.

Fig. 10 presents the best phase sensitivity  $\Delta\phi_{\min}$  of the interferometer and the corresponding supersensitive phase range as functions of the parametric gain of the second amplifier for the gain of the first amplifier and the internal losses given by (16) and for  $\Delta N_d = 100$  photons. The optimal phase sensitivity is not always obtained for the same working point, it depends on the gains of the amplifiers and losses. It is nevertheless in the dark fringe region of the interferometer for which the photon noise is minimized (see Fig. 9). It is interesting to note that the balanced case  $|r_1| = |r_2| = 1.15$  does not provide phase supersensitivity even for  $\eta = 1$ . However, the sensitivity improves as one increases the gain  $r_2$  of the second amplifier.

## VI. COMPARISON BETWEEN DIFFERENT INTERFEROMETERS AND MEASUREMENTS SCHEMES

Finally, in Fig.11 we summarize our findings and compare the different schemes studied previously. In both panels, red dashed line represents the SU(2) interferometer with homodyne detection, black solid line, the seeded SU(1,1) interferometer with homodyne detection, and red dotted line, the seeded SU(1,1) interferometer with direct detection. In all cases, the gain of the second amplifier is  $|r_2| = 3$ , the internal transmission  $\mu = 0.9$ , and the external transmission  $\eta = 0.3$ .

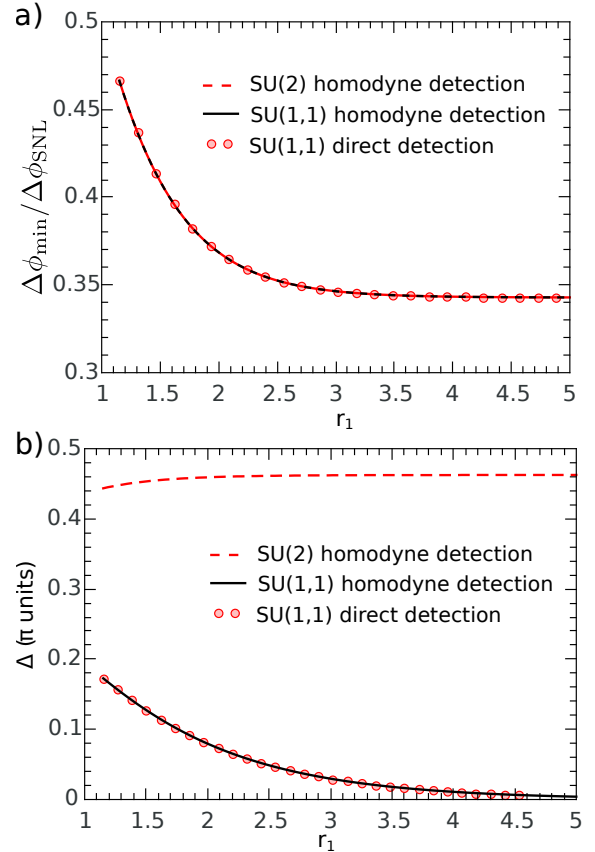


FIG. 11. Optimal phase sensitivity and the supersensitive phase range of a seeded SU(1,1) interferometer with direct (red circles) and homodyne (solid black line) detection compared to a seeded SU(2) interferometer (dashed red line). The optimal sensitivity  $\Delta\phi_{\min}$  normalized to  $\Delta\phi_{\text{SNL}}$  (a) and the supersensitive phase range (b) versus the gain  $r_1$  of the first amplifier. The gain of the second amplifier is  $|r_2| = 3$ , the internal transmission  $\mu = 0.90$ , and the external transmission  $\eta = 0.3$  in all cases.

Panel a shows the best sensitivity  $\Delta\phi_{\min}$  normalized to  $\Delta\phi_{\text{SNL}}$  and panel b, the supersensitive phase range against the parametric gain of the first amplifier. As expected from Eqs. (5)-(7) and Eq. (26), the optimal sensitivity  $\Delta\phi_{\min}$  can be improved by increasing the gain of the first amplifier for both SU(1,1) and SU(2) interferometers in all detection cases, see Fig.11a. Concerning the supersensitive phase range in Fig.11b, one can see that increasing the parametric gain of the first amplifier degrades the supersensitive phase range for

the SU(1,1) interferometer (red dots and solid black line) conversely to the SU(2) interferometer. Indeed, the supersensitive phase range is dependent on  $r_1$  in the SU(1,1) case as already noticed in Section III, Eq. (20).

## VII. CONCLUSION

We have studied the phase sensitivity properties of an SU(1,1) interferometer, considering the cases of both direct and homodyne detection at the output and taking into account internal and external losses as well as the detector noise. We have shown that the balanced configuration of an SU(1,1) interferometer, commonly considered in the literature, in which the parametric gain values of both amplifiers are equal, is not the optimal one. Increasing the gain of the second parametric amplifier always leads to a better sensitivity and a broader super-sensitive phase range. At a given gain of the first amplifier, a sufficiently large gain of the second amplifier can fully compensate for the detection losses. Although the gain unbalancing can be problematic for a FWM-based SU(1,1) interferometer because of the mode mismatch, it can be realized with high-gain parametric down conversion.

The ‘standard’ configuration of an SU(1,1) interferometer, as proposed originally and used further in experiments, is based on two non-degenerate parametric amplifiers. We have shown that its operation is similar to the one of two independent degenerate SU(1,1) interferometers. In an experiment, the non-degenerate configuration is equivalent to the degenerate one as long as one measures the sum of signal and idler parameters (quadratures or photon numbers).

We have also considered the unbalanced configuration of a linear (SU(2)) interferometer preceded by a squeezer and followed by an anti-squeezer. This case can be particularly interesting for gravitational-wave detectors where an existing SU(2) interferometer with squeezed input can be additionally equipped with an anti-squeezer at the output. We have shown that an increase in the parametric gain of this additional anti-squeezer will considerably improve the phase sensitivity. In particular, at any value of external (detection) losses, a sufficient gain of this anti-squeezer will allow one to retrieve the phase sensitivity corresponding to the case of lossless detection.

## VIII. ACKNOWLEDGEMENTS

This work was supported by the joint DFG-RFBR project CH 1591/2 – 1/16 – 52 – 12031 NNIO a. The work of F.K. was supported by LIGO NSF Grant No PHY-1305863 and Russian Foundation for Basic Research Grants No. 14 – 02 – 00399 and 16 – 52 – 10069.

### Appendix A: Notations and the quadrature operators

The annihilation operators are denoted by Roman letters  $\hat{a}, \hat{b}$ , etc. The corresponding cosine and sine quadrature

operators<sup>33,34</sup> are defined as

$$\hat{a}^c = \frac{\hat{a} + \hat{a}^\dagger}{\sqrt{2}}, \quad \hat{a}^s = \frac{\hat{a} - \hat{a}^\dagger}{i\sqrt{2}}. \quad (\text{A1})$$

The two-component quadrature vectors are denoted by the boldface Roman letters:

$$\hat{\mathbf{a}} = \begin{pmatrix} \hat{a}^c \\ \hat{a}^s \end{pmatrix}, \quad (\text{A2})$$

We assume that all incident fields are in the coherent or vacuum state. In this case, their cosine and sine quadratures are uncorrelated noises with the uncertainties equal to 1/2.

The single-mode (degenerate) Bogolyubov (squeezing) transformation in the particular case of a real squeeze factor,

$$\hat{\mathbf{b}} = \hat{\mathbf{a}} \cosh r + \hat{\mathbf{a}}^\dagger \sinh r, \quad (\text{A3})$$

in terms of the quadrature operators has a simple form

$$\hat{\mathbf{b}} = \mathbb{S}(r)\hat{\mathbf{a}}, \quad (\text{A4})$$

$$\mathbb{S}(r) = \begin{pmatrix} e^r & 0 \\ 0 & e^{-r} \end{pmatrix}. \quad (\text{A5})$$

The two-mode (non-degenerate) squeezing transformation has the form

$$\hat{\mathbf{b}}_s = \hat{\mathbf{a}}_s \cosh r + \hat{\mathbf{a}}_i^\dagger \sinh r, \quad \hat{\mathbf{b}}_i = \hat{\mathbf{a}}_i \cosh r + \hat{\mathbf{a}}_s^\dagger \sinh r, \quad (\text{A6})$$

where s,i stand for the ‘‘signal’’ and ‘‘idler’’ modes. By introducing the symmetric and antisymmetric modes,

$$\hat{\mathbf{a}}_+ = \frac{\hat{\mathbf{a}}_s + \hat{\mathbf{a}}_i}{2}, \quad \hat{\mathbf{a}}_- = \frac{\hat{\mathbf{a}}_s - \hat{\mathbf{a}}_i}{2}, \quad (\text{A7})$$

and similarly for  $\hat{\mathbf{b}}$ , it can be reduced to two independent single-mode transformations:

$$\hat{\mathbf{b}}_\pm = \hat{\mathbf{a}}_\pm \cosh r \pm \hat{\mathbf{a}}_\pm^\dagger \sinh r. \quad (\text{A8})$$

The phase shift transformation,

$$\hat{\mathbf{b}} = \hat{\mathbf{a}} e^{-i\phi}, \quad (\text{A9})$$

correspondingly, has the form

$$\hat{\mathbf{b}} = \mathbb{O}(\phi)\hat{\mathbf{a}}, \quad (\text{A10})$$

where

$$\mathbb{O}(\phi) = \begin{pmatrix} \cos \phi & \sin \phi \\ -\sin \phi & \cos \phi \end{pmatrix} = \mathbb{I} \cos \phi - \mathbb{Y} \sin \phi, \quad (\text{A11})$$

$$\mathbb{I} = \begin{pmatrix} 1 & 0 \\ 0 & 1 \end{pmatrix}, \quad \mathbb{Y} = \begin{pmatrix} 0 & -1 \\ 1 & 0 \end{pmatrix}. \quad (\text{A12})$$

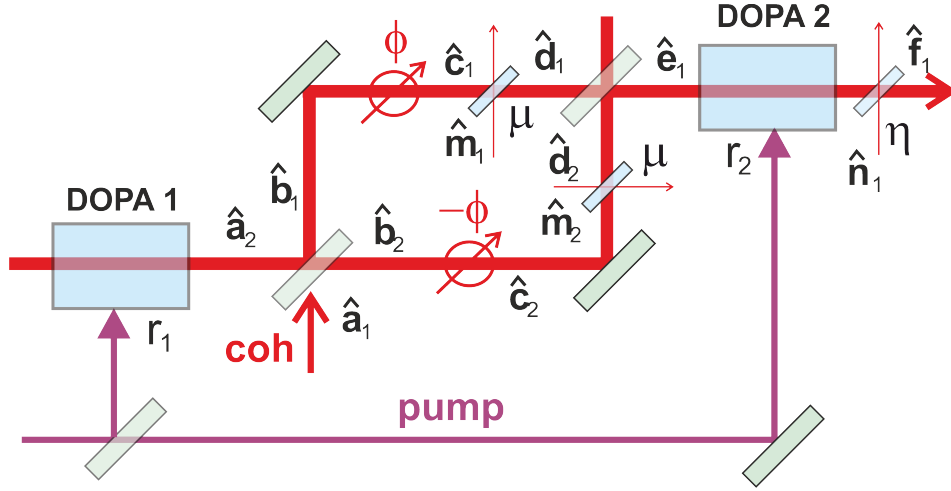


FIG. 12. A linear interferometer preceded by a squeezer (degenerate optical parametric amplifier, DOPA1, with a squeeze factor of  $r_1$ , and followed by an anti-squeezer (DOPA2), with the squeeze factor  $r_2$ . The figure shows the notation used in the calculations. The pumping is depicted schematically.

## Appendix B: Linear interferometer

### 1. Field transformations in the interferometer

The two-component quadrature vectors of the incident fields (see Fig. 12) are  $\hat{\mathbf{a}}_1, \hat{\mathbf{a}}_2$ . The first beamsplitter transforms them into

$$\hat{\mathbf{b}}_1 = \frac{\hat{\mathbf{a}}_1 + \hat{\mathbf{a}}_2}{\sqrt{2}}, \quad \hat{\mathbf{b}}_2 = \frac{\hat{\mathbf{a}}_1 - \hat{\mathbf{a}}_2}{\sqrt{2}}. \quad (\text{B1})$$

The phase shift gives, correspondingly,

$$\hat{\mathbf{c}}_1 = \frac{\mathbb{O}(\phi)(\hat{\mathbf{a}}_1 + \hat{\mathbf{a}}_2)}{\sqrt{2}}, \quad \hat{\mathbf{c}}_2 = \frac{\mathbb{O}(-\phi)(\hat{\mathbf{a}}_1 - \hat{\mathbf{a}}_2)}{\sqrt{2}}. \quad (\text{B2})$$

We model internal losses by an imaginary beam splitter with the power transmissivity  $\mu$ , which gives

$$\begin{aligned} \hat{\mathbf{d}}_1 &= \sqrt{\frac{\mu}{2}} \mathbb{O}(\phi)(\hat{\mathbf{a}}_1 + \hat{\mathbf{a}}_2) + \sqrt{1-\mu} \hat{\mathbf{m}}_1, \\ \hat{\mathbf{d}}_2 &= \sqrt{\frac{\mu}{2}} \mathbb{O}(-\phi)(\hat{\mathbf{a}}_1 - \hat{\mathbf{a}}_2) + \sqrt{1-\mu} \hat{\mathbf{m}}_2, \end{aligned} \quad (\text{B3})$$

where  $\hat{\mathbf{m}}_{1,2}$  are the corresponding introduced vacuum noises. At one of the outputs of the second beamsplitter, we have

$$\hat{\mathbf{e}}_1 = \frac{\hat{\mathbf{d}}_1 - \hat{\mathbf{d}}_2}{\sqrt{2}} = \sqrt{\mu}(\hat{\mathbf{a}}_2 \cos \phi - \mathbb{Y} \hat{\mathbf{a}}_1 \sin \phi) + \sqrt{1-\mu} \hat{\mathbf{m}}_-, \quad (\text{B4})$$

where

$$\hat{\mathbf{m}}_- = \frac{\hat{\mathbf{m}}_1 - \hat{\mathbf{m}}_2}{\sqrt{2}}. \quad (\text{B5})$$

Finally, the second squeezer and the output losses give

$$\begin{aligned} \hat{\mathbf{f}}_1 &= \sqrt{\eta} \mathbb{S}(r_2) \hat{\mathbf{e}}_1 + \sqrt{1-\eta} \hat{\mathbf{n}}_1 \\ &= \sqrt{\eta} \mathbb{S}(r_2) [\sqrt{\mu}(\hat{\mathbf{a}}_2 \cos \phi - \mathbb{Y} \hat{\mathbf{a}}_1 \sin \phi) + \sqrt{1-\mu} \hat{\mathbf{m}}_-] \\ &\quad + \sqrt{1-\eta} \hat{\mathbf{n}}_1, \end{aligned} \quad (\text{B6})$$

where  $\eta$  is the power transmissivity of the imaginary beam splitter that models the output losses, and  $\hat{\mathbf{n}}_1$  is the added vacuum noise.

### 2. Homodyne detection

Let there be coherent light at input 1, and squeezed vacuum at input 2:

$$\begin{aligned} \hat{\mathbf{a}}_1 &= \begin{pmatrix} \sqrt{2} \alpha \\ 0 \end{pmatrix} + \hat{\mathbf{z}}_1, \\ \hat{\mathbf{a}}_2 &= \mathbb{S}(r_1) \hat{\mathbf{z}}_2, \end{aligned} \quad (\text{B7})$$

where  $\hat{\mathbf{z}}_{1,2}$  are vacuum fields. In this case,

$$\hat{\mathbf{f}}_1^c = \frac{\sqrt{\mu\eta} [\hat{z}_2^c e^{-r_1} \cos \phi + \hat{z}_1^s \sin \phi] e^{-r_2}}{\sqrt{(1-\mu)\eta} \hat{m}_-^c e^{-r_2} + \sqrt{1-\eta} \hat{n}_1^c}, \quad (\text{B8})$$

$$\hat{\mathbf{f}}_1^s = \frac{\sqrt{\mu\eta} [\hat{z}_2^s e^{-r_1} \cos \phi - (\sqrt{2} \alpha + \hat{z}_1^c) \sin \phi] e^{-r_2}}{\sqrt{(1-\mu)\eta} \hat{m}_-^s e^{-r_2} + \sqrt{1-\eta} \hat{n}_1^s}. \quad (\text{B9})$$

One can see that if  $|\phi| \ll 1$ , then the sine quadrature contains the most significant part of the phase information (the term  $\sqrt{2} \alpha \sin \phi$ ). Therefore, assume that it is this quadrature that is measured by a homodyne detector. It follows from (B9) that the mean value and the uncertainty of  $\hat{\mathbf{f}}_1^s$  are

$$\langle \hat{\mathbf{f}}_1^s \rangle = -\sqrt{2\mu\eta} \alpha e^{-r_2} \sin \phi, \quad (\text{B10})$$

$$\begin{aligned} (\Delta \hat{\mathbf{f}}_1^s)^2 &= \langle (\hat{\mathbf{f}}_1^s - \langle \hat{\mathbf{f}}_1^s \rangle)^2 \rangle \\ &= \frac{1}{2} [\mu\eta (e^{-2r_1} \cos^2 \phi + \sin^2 \phi) e^{-2r_2} + (1-\mu)\eta e^{-2r_2} + 1-\eta]. \end{aligned} \quad (\text{B11})$$

The phase measurement error is defined by

$$(\Delta\phi)^2 = \frac{(\Delta\hat{f}_1^s)^2}{\left(\frac{\partial\langle\hat{f}_1^s\rangle}{\partial\phi}\right)^2}, \quad (\text{B12})$$

which gives Eqs. (5-7).

### Appendix C: Degenerate SU(1,1) interferometer

#### 1. Field transformations

Here, we repeat the calculations of B 1 for the case of a degenerate SU(1,1) interferometer. The scheme with the main notation is shown in Fig. 13.

The two-components quadrature vector  $\hat{\mathbf{a}}$  for the incident field becomes, after the first DOPA,

$$\hat{\mathbf{b}} = \mathbb{S}(r_1)\hat{\mathbf{a}}. \quad (\text{C1})$$

After the signal phase shift, it becomes

$$\hat{\mathbf{c}} = \mathbb{O}(\phi)\hat{\mathbf{b}}. \quad (\text{C2})$$

The internal losses are taken into account by the effective beamsplitter transformation,

$$\hat{\mathbf{d}} = \sqrt{\mu}\hat{\mathbf{b}} + \sqrt{1-\mu}\hat{\mathbf{m}}. \quad (\text{C3})$$

After the second DOPA, the quadrature vector becomes

$$\hat{\mathbf{e}} = \mathbb{S}(r_2)\hat{\mathbf{d}}. \quad (\text{C4})$$

The external losses are taken into account by the effective beamsplitter transformation,

$$\begin{aligned} \hat{\mathbf{f}} &= \sqrt{\eta}\hat{\mathbf{e}} + \sqrt{1-\eta}\hat{\mathbf{n}} \\ &= \sqrt{\eta}\mathbb{S}(r_2)\left[\sqrt{\mu}\mathbb{O}(\phi)\mathbb{S}(r_1)\hat{\mathbf{a}} + \sqrt{1-\mu}\hat{\mathbf{m}}\right] + \sqrt{1-\eta}\hat{\mathbf{n}}. \end{aligned} \quad (\text{C5})$$

In the case of a coherent seed beam at the input of the first DOPA (Fig. 13), the quadrature vector has the form

$$\hat{\mathbf{a}} = \boldsymbol{\zeta} + \hat{\mathbf{z}}, \quad (\text{C6})$$

where  $\hat{\mathbf{z}}$  is a vacuum field and  $\boldsymbol{\zeta}$  is the seed quadratures vector. In this case,

$$\hat{\mathbf{b}} = \mathbb{S}(r_1)\hat{\mathbf{a}}. \quad (\text{C7})$$

$$\hat{\mathbf{f}} = \sqrt{\eta}\mathbb{S}(r_2)\left\{\sqrt{\mu}\mathbb{O}(\phi)\left[\boldsymbol{\alpha} + \mathbb{S}(r_1)\hat{\mathbf{a}}\right] + \sqrt{1-\mu}\hat{\mathbf{m}}\right\} + \sqrt{1-\eta}\hat{\mathbf{n}}, \quad (\text{C8})$$

where

$$\boldsymbol{\alpha} = \mathbb{S}(r_1)\boldsymbol{\zeta} = |\alpha| \begin{pmatrix} \cos\psi \\ -\sin\psi \end{pmatrix} \quad (\text{C9})$$

is the seed quadratures vector inside the interferometer. (Please note that here,  $\alpha$  depends on  $r_1$ .)

#### 2. Seeded case with homodyne detection

Here we suppose that the phase of the coherent seed is equal to zero:

$$\boldsymbol{\alpha} = \begin{pmatrix} \sqrt{2}\alpha \\ 0 \end{pmatrix}. \quad (\text{C10})$$

In this case,

$$\hat{f}^c = \sqrt{\mu\eta}\left[(\sqrt{2}\alpha + \hat{z}^c e^{r_1})\cos\phi + \hat{z}^s e^{-r_1}\sin\phi\right]e^{r_2} + \sqrt{(1-\mu)\eta}\hat{m}^c e^{r_2} + \sqrt{1-\eta}\hat{n}^c, \quad (\text{C11})$$

$$\hat{f}^s = \sqrt{\mu\eta}\left[\hat{z}^s e^{-r_1}\cos\phi - (\sqrt{2}\alpha + \hat{z}^c e^{r_1})\sin\phi\right]e^{-r_2} + \sqrt{(1-\mu)\eta}\hat{m}^s e^{-r_2} + \sqrt{1-\eta}\hat{n}^s, \quad (\text{C12})$$

As in B, at  $|\phi| \ll 1$  the sine quadrature contains the most significant part of the phase information (the term  $\sqrt{2}\alpha\sin\phi$ ). It follows from (C12) that the mean value and the variance of  $\hat{f}^s$  are

$$\langle\hat{f}^s\rangle = -\sqrt{2\mu\eta}\alpha e^{-r_2}\sin\phi, \quad (\text{C13})$$

$$\begin{aligned} (\Delta\hat{f}^s)^2 &= \langle(\hat{f}^s - \langle\hat{f}^s\rangle)^2\rangle \\ &= \frac{1}{2}\left[\mu\eta(e^{-2r_1}\cos^2\phi + e^{2r_1}\sin^2\phi)e^{-2r_2} + (1-\mu)\eta e^{-2r_2} + 1 - \eta\right]. \end{aligned} \quad (\text{C14})$$

The phase measurement error is defined by

$$(\Delta\phi)^2 = \frac{(\Delta\hat{f}^s)^2}{\left(\frac{\partial\langle\hat{f}^s\rangle}{\partial\phi}\right)^2}, \quad (\text{C15})$$

which gives Eqs. (5, 6, 19).

#### 3. Seeded case with direct detection

Let us rewrite Eq (C8) back in the annihilation/creation operator notation:

$$\hat{f} = \sqrt{\mu\eta}\theta(\phi) + \hat{f}_{\text{fl}}, \quad (\text{C16})$$

where

$$\theta(\phi) = \alpha e^{-i\phi}\cosh r_2 + \alpha^* e^{i\phi}\sinh r_2, \quad (\text{C17})$$

$$\alpha = |\alpha|e^{-i\psi}, \quad (\text{C18})$$

$$\hat{f}_{\text{fl}} = \sqrt{\mu\eta}\left[C(\phi)\hat{\mathbf{a}} + S(\phi)\hat{\mathbf{a}}^\dagger\right] + \sqrt{\eta(1-\mu)}(\hat{m}\cosh r_2 + \hat{m}^\dagger\sinh r_2) + \sqrt{1-\eta}\hat{\mathbf{n}}, \quad (\text{C19})$$

$$\begin{aligned} C(\phi) &= \cosh r_1 \cosh r_2 e^{-i\phi} + \sinh r_1 \sinh r_2 e^{i\phi}, \\ S(\phi) &= \sinh r_1 \cosh r_2 e^{-i\phi} + \cosh r_1 \sinh r_2 e^{i\phi}. \end{aligned} \quad (\text{C20})$$

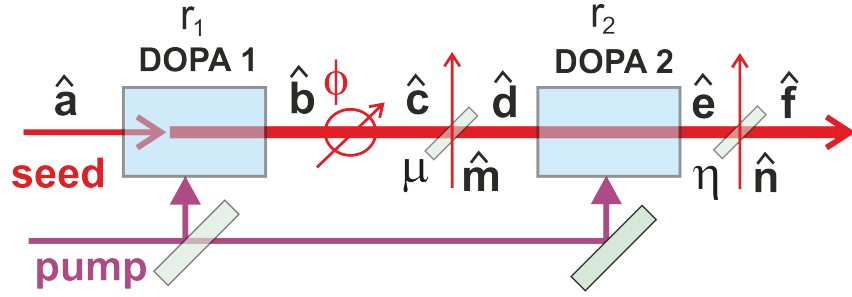


FIG. 13. Degenerate SU(1,1) interferometer and the notation used in the calculations. The pumping of the DOPAs is shown schematically.

The number of quanta on the detector, up to small second-order terms, is equal to

$$\hat{N}_f = \hat{f}^\dagger \hat{f} = \langle \hat{N}_f \rangle + \delta \hat{N}_f, \quad (\text{C21})$$

where

$$\langle \hat{N}_f \rangle = \mu \eta |\theta(\phi)|^2 = \mu \eta |\alpha|^2 [\cosh 2r_2 + \sinh 2r_2 \cos 2(\phi + \psi)], \quad (\text{C22})$$

$$\delta \hat{N}_f = \sqrt{\mu \eta} [\theta(\phi) \hat{f}_{\text{fl}}^\dagger + \theta^*(\phi) \hat{f}_{\text{fl}}]. \quad (\text{C23})$$

are the mean number and the variance of  $\hat{N}_f$ . Therefore,

$$(\Delta N_f)^2 = \langle (\delta \hat{N}_f)^2 \rangle = \mu \eta |\alpha|^2 [\mu \eta \sigma_a^2 + (1 - \mu) \eta \sigma_m^2 + (1 - \eta) \sigma_n^2], \quad (\text{C24})$$

and

$$(\Delta \phi)^2 = \frac{(\Delta N_f)^2}{\left( \frac{\partial \langle N_f \rangle}{\partial \phi} \right)^2} = \frac{\sigma_a^2 + \frac{1 - \mu}{\mu} \sigma_m^2 + \frac{1 - \eta}{\mu \eta} \sigma_n^2}{4 |\alpha|^2 \sinh^2 2r_2 \sin^2 2(\phi + \psi)}, \quad (\text{C25})$$

where

$$\sigma_n^2 = e^{2r_2} \cos^2(\phi + \psi) + e^{-2r_2} \sin^2(\phi + \psi), \quad (\text{C26})$$

$$\sigma_m^2 = e^{4r_2} \cos^2(\phi + \psi) + e^{-4r_2} \sin^2(\phi + \psi), \quad (\text{C27})$$

$$\sigma_a^2 = \cosh 2r_1 \cosh 4r_2 + \sinh 2r_1 [\cosh 4r_2 \cos 2\phi \cos 2(\phi + \psi) + \sin 2\phi \sin 2(\phi + \psi)] + [\cosh 2r_1 \cos 2(\phi + \psi) + \sinh 2r_1 \cos 2\phi] \sinh 4r_2, \quad (\text{C28})$$

and

$$\frac{\partial \langle N_f \rangle}{\partial \phi} = -2\mu \eta |\alpha|^2 \sinh 2r_2 \sin 2(\phi + \psi). \quad (\text{C29})$$

Numerical optimization shows that if  $e^{r_1} \gg 1$ ,  $e^{-r_2} \gg 1$ , then the optimal values of  $\phi$ ,  $\psi$  are close to 0. In this case,

$$\sigma_n^2 = e^{-2|r_2|} + e^{2|r_2|} (\phi + \psi)^2, \quad (\text{C30})$$

$$\sigma_m^2 = e^{-4|r_2|} + e^{4|r_2|} (\phi + \psi)^2, \quad (\text{C31})$$

$$\sigma_a^2 = e^{-4|r_2| + 2r_1} + 2e^{2r_1} \phi (\phi + \psi) + e^{4|r_2|} (e^{2r_1} \phi^2 + e^{-2r_1}) (\phi + \psi)^2, \quad (\text{C32})$$

and

$$\frac{\partial \langle N_f \rangle}{\partial \phi} = 2\mu \eta |\alpha|^2 e^{2|r_2|} (\phi + \psi), \quad (\text{C33})$$

The minimum of (C32) in  $\phi$  is at

$$\phi = -\frac{e^{-4|r_2|}}{\phi + \psi} \quad (\text{C34})$$

and is equal to

$$\sigma_a^2 = e^{4|r_2| - 2r_1} (\phi + \psi)^2. \quad (\text{C35})$$

#### 4. Unseeded case with direct detection

If  $\alpha = 0$ , then  $\hat{f} = \hat{f}_{\text{fl}}$  [see Eq. (C19)], and the mean value and the variance of the number of quanta at the output are equal to

$$\langle \hat{N}_f \rangle = \langle \hat{f}^\dagger \hat{f} \rangle = \eta [\mu |S(\phi)|^2 + (1 - \mu) \sinh^2 r_2], \quad (\text{C36})$$

$$\begin{aligned} (\Delta N_f)^2 &= \langle \hat{N}_f^2 \rangle - \langle \hat{N}_f \rangle^2 \\ &= \eta^2 \{ \mu^2 |S(\phi)|^2 [ |C(\phi)|^2 + |S(\phi)|^2 ] \\ &\quad + 2\mu(1 - \mu) |S(\phi)|^2 \sinh^2 r_2 + (1 - \mu)^2 \sinh^2 r_2 \cosh 2r_2 \} \\ &\quad + \langle \hat{N}_f \rangle. \end{aligned} \quad (\text{C37})$$

Due to the losses in a realistic interferometer, as well as this additional measurement error, a good phase sensitivity can be evidently achieved only if

$$\langle N_f \rangle \gg 1. \quad (\text{C38})$$

In this case, the discrete value of  $N_f$  can be approximated by continuous one, and the phase measurement error can be calculated as

$$(\Delta \phi)^2 = \frac{(\Delta N_f)^2 + (\Delta N_d)^2}{\left( \frac{\partial \langle N_f \rangle}{\partial \phi} \right)^2}, \quad (\text{C39})$$

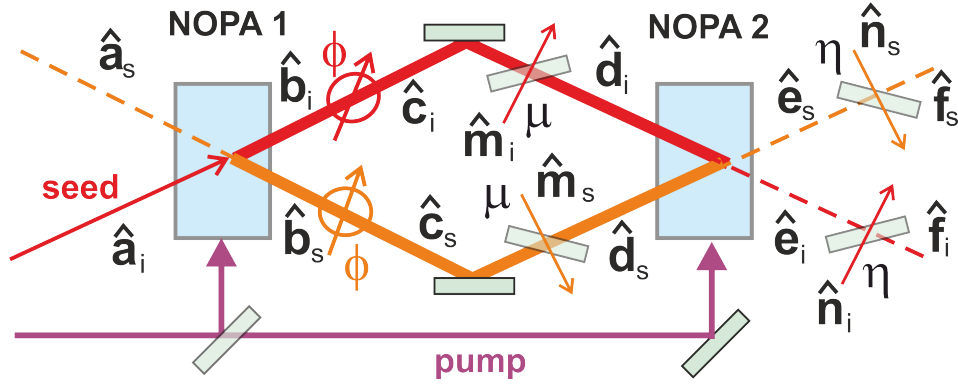


FIG. 14. A non-degenerate SU(1,1) interferometer with the notation used in the calculations. The pumping is depicted schematically.

where [see Eqs. (C20), (C36)]

$$\frac{\partial \langle N_f \rangle}{\partial \phi} = -\mu \eta \sinh 2r_1 \sinh 2r_2 \sin 2\phi \quad (\text{C40})$$

where  $\Delta N_d \gg 1$  is the additional detection error which we take into account in this particular case due to the relatively small number of photons measured by the detector. Therefore,

$$(\Delta \phi)^2 = \frac{2|C(\phi)|^2 |S(\phi)|^2 + A|S(\phi)|^2 + B}{\sinh^2 2r_1 \sinh^2 2r_2 \sin^2 2\phi}, \quad (\text{C41})$$

where

$$\begin{aligned} A &= 2 \frac{1-\mu}{\mu} \sinh^2 r_2 + \frac{1-\mu\eta}{\mu\eta}, \\ B &= \frac{1-\mu}{\mu} \sinh^2 r_2 \left( A + \frac{1}{\mu} \right) + \frac{(\Delta N_d)^2}{\mu^2 \eta^2}. \end{aligned} \quad (\text{C42})$$

#### Appendix D: Non-degenerate SU(1,1) interferometer

We now repeat the calculations of B 1 for the case of a non-degenerate SU(1,1) interferometer (Fig. 14). The incident fields are  $\hat{\mathbf{a}}_s, \hat{\mathbf{a}}_i$ , with the subscripts  $s$  and  $i$  corresponding to the signal and idler modes. The first NOPA transforms them as

$$\hat{\mathbf{b}}_s = \hat{\mathbf{a}}_s \cosh r_1 + \mathbb{Z} \hat{\mathbf{a}}_i \sinh r_1, \quad \hat{\mathbf{b}}_i = \hat{\mathbf{a}}_i \cosh r_1 + \mathbb{Z} \hat{\mathbf{a}}_s \sinh r_1, \quad (\text{D1})$$

where

$$\mathbb{Z} = \begin{pmatrix} 1 & 0 \\ 0 & -1 \end{pmatrix}. \quad (\text{D2})$$

After the phase shift (equal in signal and idler arms), they become

$$\hat{\mathbf{c}}_s = \mathbb{O}(\phi) \hat{\mathbf{b}}_s, \quad \hat{\mathbf{c}}_i = \mathbb{O}(\phi) \hat{\mathbf{b}}_i. \quad (\text{D3})$$

The internal losses, also the same in both arms, give

$$\hat{\mathbf{d}}_s = \sqrt{\mu} \hat{\mathbf{b}}_s + \sqrt{1-\mu} \hat{\mathbf{m}}_s, \quad \hat{\mathbf{d}}_i = \sqrt{\mu} \hat{\mathbf{b}}_i + \sqrt{1-\mu} \hat{\mathbf{m}}_i. \quad (\text{D4})$$

After the second NOPA, the quadrature vectors become

$$\hat{\mathbf{e}}_s = \hat{\mathbf{d}}_s \cosh r_2 + \mathbb{Z} \hat{\mathbf{d}}_i \sinh r_2, \quad \hat{\mathbf{e}}_i = \hat{\mathbf{d}}_i \cosh r_2 + \mathbb{Z} \hat{\mathbf{d}}_s \sinh r_2. \quad (\text{D5})$$

Finally, the external losses give

$$\hat{\mathbf{f}}_s = \sqrt{\eta} \hat{\mathbf{e}}_s + \sqrt{1-\eta} \hat{\mathbf{n}}_s, \quad \hat{\mathbf{f}}_i = \sqrt{\eta} \hat{\mathbf{e}}_i + \sqrt{1-\eta} \hat{\mathbf{n}}_i. \quad (\text{D6})$$

Now introduce the symmetric and antisymmetric modes,

$$\hat{\mathbf{a}}_{\pm} = \frac{\hat{\mathbf{a}}_s \pm \hat{\mathbf{a}}_i}{\sqrt{2}}, \quad \hat{\mathbf{b}}_{\pm} = \frac{\hat{\mathbf{b}}_s \pm \hat{\mathbf{b}}_i}{\sqrt{2}}, \quad (\text{D7})$$

and similarly for  $\hat{\mathbf{b}}_{i,s} \dots \hat{\mathbf{f}}_{i,s}, \hat{\mathbf{m}}_{i,s}, \hat{\mathbf{n}}_{i,s}$ . Equations for these modes, which can be obtained from (D1-D6), are identical to the equations for the degenerate case, with the only exception that the squeeze factors for the “-” mode are equal to  $-r_1, -r_2$ . Note that if all incident fields in Eqs.(D1-D6) are uncorrelated, then the same is true for the “ $\pm$ ” fields. Therefore, the non-degenerate interferometer is equivalent to two independent degenerate ones.

Note also that in each “cross-section” of the original non-degenerate interferometer, the total number of quanta in the signal and idler beams is equal to the total number of quanta in the corresponding “cross-section” of the equivalent degenerate interferometers, *e.g.*,

$$\hat{\mathbf{b}}_s^\dagger \hat{\mathbf{b}}_s + \hat{\mathbf{b}}_i^\dagger \hat{\mathbf{b}}_i = \hat{\mathbf{b}}_+^\dagger \hat{\mathbf{b}}_+ + \hat{\mathbf{b}}_-^\dagger \hat{\mathbf{b}}_-, \quad (\text{D8})$$

$$\hat{\mathbf{f}}_s^\dagger \hat{\mathbf{f}}_s + \hat{\mathbf{f}}_i^\dagger \hat{\mathbf{f}}_i = \hat{\mathbf{f}}_+^\dagger \hat{\mathbf{f}}_+ + \hat{\mathbf{f}}_-^\dagger \hat{\mathbf{f}}_-. \quad (\text{D9})$$

#### REFERENCES



- 
- <sup>1</sup> Abbott B. *et al* (LIGO Scientific Collaboration and Virgo Collaboration), *Phys. Rev. Lett.* **116**, 061102 (2016).
- <sup>2</sup> This value differs from the one frequently found in the literature by the factor  $1/2$ . The same is true for the Heisenberg limit (2) and other equations for the phase sensitivity in two-arm schemes. This factor arises because we define the relative phase shift in a two-arm scheme as  $2\phi$ . This definition provides more consistent equations for the two- and single-arm cases.
- <sup>3</sup> W. Heitler, *The Quantum Theory of Radiation*, 3rd ed. (Clarendon Press, 1954).
- <sup>4</sup> Strictly speaking, this “proof” is incorrect, because (i) a “well-behaved” phase operator can not be defined<sup>35</sup> and (ii) there exist probability distributions with  $\Delta N \gg N$ . Nevertheless, substitutes of the phase operator are proposed which give the same result (3) provided that  $\Delta\phi \ll 1$ <sup>35–38</sup>.
- <sup>5</sup> C. Helstrom, *Quantum Detection and Estimation Theory* (Academic Press, 1976).
- <sup>6</sup> C. M. Caves, *Phys. Rev. D* **23**, 1693 (1981).
- <sup>7</sup> B. Yurke, S. L. McCall, and J. R. Klauder, *Phys. Rev. A* **33**, 4033 (1986).
- <sup>8</sup> S. L. Braunstein and C. M. Caves, *Physical Review Letters* **72**, 3439 (1994).
- <sup>9</sup> L. Pezzé and A. Smerzi, *Physical review letters* **100**, 073601 (2008).
- <sup>10</sup> M. J. Holland and K. Burnett, *Phys. Rev. Lett.* **71**, 1355 (1993).
- <sup>11</sup> H. Lee, P. Kok, and J. P. Dowling, *Journal of Modern Optics* **49**, 2325 (2002).
- <sup>12</sup> Abadie J. *et al*, *Nature Physics* **7**, 962 (2011).
- <sup>13</sup> <http://www.geo600.org>.
- <sup>14</sup> Aasi J *et al*, *Nature Photonics* **7**, 613 (2013).
- <sup>15</sup> M. Chekhova and Z. Ou, *Advances in Optics and Photonics* **8**, 104 (2016).
- <sup>16</sup> W. N. Plick, J. P. Dowling, and G. S. Agarwal, *New Journal of Physics* **12**, 083014 (2010).
- <sup>17</sup> A. M. Marino, N. V. Corzo Trejo, and P. D. Lett, *Phys. Rev. A* **86**, 023844 (2012).
- <sup>18</sup> J. Jing, C. Liu, Z. Zhou, Z. Y. Ou, and W. Zhang, *Applied Physics Letters* **99**, 011110 (2011), 10.1063/1.3606549.
- <sup>19</sup> J. Kong, J. Jing, H. Wang, F. Hudelist, C. Liu, and W. Zhang, *Applied Physics Letters* **102**, 011130 (2013), 10.1063/1.4774380.
- <sup>20</sup> F. Hudelist, J. Kong, C. Liu, J. Jing, Z. Ou, and W. Zhang, *Nature Communications* **5**, 3049 (2014).
- <sup>21</sup> H. Wang, A. M. Marino, and J. Jing, *Applied Physics Letters* **107**, 121106 (2015), 10.1063/1.4931686.
- <sup>22</sup> N. Liu, Y. Liu, X. Guo, L. Yang, X. Li, and Z. Ou, *Opt. Express* **24**, 1096 (2016).
- <sup>23</sup> P. Sharapova, A. M. Pérez, O. V. Tikhonova, and M. V. Chekhova, *Phys. Rev. A* **91**, 043816 (2015).
- <sup>24</sup> T. S. Iskhakov, A. M. Pérez, K. Y. Spasibko, M. V. Chekhova, and G. Leuchs, *Opt. Lett.* **37**, 1919 (2012).
- <sup>25</sup> A. M. Pérez, T. S. Iskhakov, P. Sharapova, S. Lemieux, O. V. Tikhonova, M. V. Chekhova, and G. Leuchs, *Opt. Lett.* **39**, 2403 (2014).
- <sup>26</sup> D. Li, C.-H. Yuan, Z. Y. Ou, and W. Zhang, *New Journal of Physics* **16**, 073020 (2014).
- <sup>27</sup> R. Demkowicz-Dobrzanski, M. Jarzyna, and J. Kolodynski, in *Progress in Optics*, Vol. 60, edited by E. Wolf (Elsevier, 2015) pp. 345–435.
- <sup>28</sup> M. Jarzyna and R. Demkowicz-Dobrzański, *Phys. Rev. A* **85**, 011801 (2012).
- <sup>29</sup> S. Knysh, V. N. Smelyanskiy, and G. A. Durkin, *Phys. Rev. A* **83**, 021804 (2011).
- <sup>30</sup> B. M. Escher, R. L. de Matos Filho, and D. L., *Nature Physics* **7**, 406 (2011), 10.1038/nphys1958.
- <sup>31</sup> R. Demkowicz-Dobrzański, J. Kolodyński, and G. Mādälin, *Nature Communications* **3**, 1063 (2012).
- <sup>32</sup> R. Demkowicz-Dobrzański, K. Banaszek, and R. Schnabel, *Phys. Rev. A* **88**, 041802 (2013).
- <sup>33</sup> C. M. Caves and B. L. Schumaker, *Phys. Rev. A* **31**, 3068 (1985).
- <sup>34</sup> B. L. Schumaker and C. M. Caves, *Phys. Rev. A* **31**, 3093 (1985).
- <sup>35</sup> P. Carruthers and M. M. Nieto, *Rev. Mod. Phys.* **40**, 411 (1968).
- <sup>36</sup> L. Susskind and J. Glogower, *Physics* **1**, 49 (1964).
- <sup>37</sup> V. Popov and V. Yarunin, *Vestn. Leningr. Univ.* **22**, 7 (1973), in Russian.
- <sup>38</sup> D. T. Pegg and S. M. Barnett, *Phys. Rev. A* **39**, 1665 (1989).